Journal Name

ARTICLE

Design and synthesis of fluorenone-based dyes: two-photon excited fluorescent probes for imaging of Lysosomes and Mitochondria in living cells

A. L. Capodilupo,[a] V. Vergaro,[a] E. Fabiano,[a,b] Milena De Giorgi,[a] F. Baldassarre,[c] A. Cadone,[d] A. Maggiore,[a] V. Maiorano,[a] D. Sanvitto,[a] G. Gigli[a,b,e] and G. Ciccarella[a,f]*

Three fluorenone-derived two-photon fluorescent probes (**TK**) targeting the lysosomes (**TK-Lyso**) and mitochondria (**TK-Mito1** and **TK-Mito2**) were synthesized by introducing different diphenylamine moieties on fluorenone-core. The **TK** dyes showed high biocompatibility and long-term retention, low cytotoxicity, large Stoke's shift and good fluorescence quantum yield. The results of the present work disclose a class of organic dyes with potential wide applications as specific and efficient lysosome and mitochondria probes in the study of various biological processes.

Introduction

A number of fluorescent small molecule probes have been developed that selectively stain organelles[1, 2] or indicate the status of cells or specific cellular components, including second messengers,[3] pH,[4] reactive oxygen species,[5] metal ions,[6] nitric oxide,[7] nucleic acids,[8] and cell differentiation.[9] Such probes have made significant contributions to biomedical research. However, many cellular components remain to be explored by small molecule probes, and the demand for reagents that specifically stain different components of living cells is increasing.[10]

Lysosomes (**Lyso**) and mitochondria (**Mito**) are two basic structural and functional organelles in eukaryotic cells. Lysosomes (**Lyso**), which are roughly spherical bodies enclosed by a single membrane, receive and degrade lipids and proteins via secretory, endocytic, autophagic, and phatocytic membrane-trafficking pathways.[11] Mitochondria, the principal energy-producing compartment in most cells, play key roles in numerous vital cellular processes.[12, 13] Thus, these organelles are crucially involved in various pathologies, from Alzheimer's disease to cancer and diabetes.[14, 15]

Consequently, lysosomes and mitochondria-staining reagents and techniques are of great importance for biomedical research[7–11] and potentially also for diagnosis.
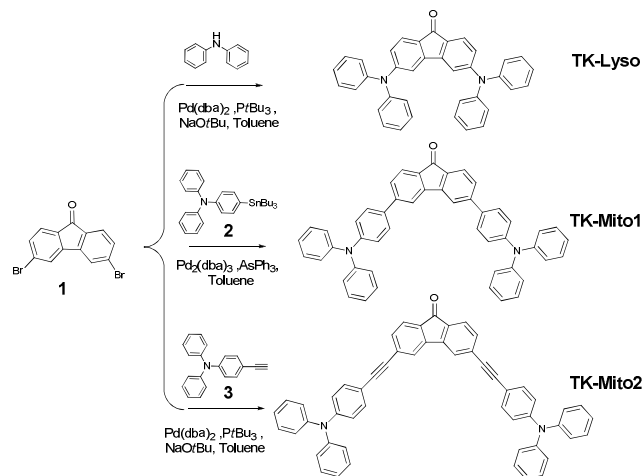
Among various conventional bioimaging techniques, the two-photon fluorescence microscopy (2PM) is a very attractive and non-invasive tool for living cell and tissue imaging.[16] In particular, 2PM, thanks to the unique characteristics of two-photon absorption process that occurs in the probes excited, i.e. long excitation wavelength (700-1000 nm) and quadratic-intensity dependence,[17] enables the high-resolution visualization of intracellular organelles in living specimens.[18] In addition, the 2PM uses low-energy near-infrared laser excitation and allow deep penetration with low photobleaching and photodamage of the tissue during the imaging. Thus, several research groups have reported a number of two-photon fluorescent probes for lysosomes based on different fluorophores.[15-17] However, two-photon fluorescent probes for mitochondria are still rare.[19-22]

This being so, a significant demand remains for lysosomes and mitochondria selective probes with high bio- and photo-stability, low cytotoxicity, large Stoke's shift, and having long-wavelength emission peaks, in order to facilitate tissue penetration.

Here we report the synthesis of a set of fluorenone-based fluorescent probes labelled as **TK** (Scheme. 1) for specific imaging of **Lyso** (**TK-Lyso**) and **Mito** (**TK-Mito1**, **TK-Mito2**) in living specimens. **TK** dyes were designed by connecting different diphenylamine units at the 3 and 6-positions of the fluorenone molecule, in order to extend the π-conjugation of the final compounds and realize push-pull systems. The **TK** dyes exhibited excellent photostability, good quantum yield, large Stokes shift (> 80 nm) and large two-photon cross-section.

The synthesized dyes showed selective localization in lysosomes (**TK-Lyso**) and mitochondria (**TK-Mito1 and TK-Mito2**), with high biocompatibility, long-term retention and pH insensitivity in the range 2-9, important features for biological applications. Furthermore, study on dependence from mitochondrial membrane potential were also carried out, showing that **TK-Mito1** and **TK-Mito2**, like MitoTracker Red, are dependent on mitochondrial membrane potential.

Scheme 1. Synthetic route to **TK** dyes.

Experimental Section

Reagents and instruments

All reactions were carried out under a nitrogen atmosphere. Solvents were freshly distilled prior to use according to standard procedures. Commercial products were purchased from Sigma-Aldrich. (**LTR**) and MitoTracker Red CMXRos (**MTR**) were purchased from Life technologies. Glass bottom Petri Dishes for confocal experiments were purchased from WillCo Dish®. The microwave used was a CEM Discover Labmate. ^{1}H and ^{13}C NMR spectra were recorded on a Bruker 400 MHz spectrometer. Splitting patterns were described as singlet (s), doublet (d), triplet (t), quartet (q), or multiplet (m). LC-MS spectra were acquired with an Agilent 6300 Series Ion Trap interfaced to an Agilent 1200 HPLC, adopting the following general conditions: atmospheric pressure chemical ionization, positive ions, eluent chloroform, flow rate 0.200 mL min-1, drying gas flow 5.0 L min-1, nebulizer pressure 60 psi, drying gas temperature 350 °C, vaporizer temperature 325 °C, mass range 100–2200 m/z.

Optical measurements

The one-photon absorption (OPA) spectra were obtained on a Varian-Cary 500 spectrophotometer. UV-Vis absorption spectra were recorded on a Varian-Cary 500 spectrophotometer. The one-photon excited fluorescence (OPEF) spectra measurements were performed using a Varian Cary Eclipse spectrofluorimeter. OPA and OPEF spectra of dyes were measured in three organic solvents of different polarities, with

the concentration of 1.0×10^{-5} M. The quartz cuvettes used were of 1 cm path length. The fluorescence quantum yields (Φ) were determined by using Tris(2,2'-bipyridyl)dichlororuthenium(II) hexahydrate [$Ru(bpy)_3$] as the reference, according to the literature method Quantum yields were collected as follows:

$$\Phi s = (A_r \eta_s^2 F_s)/A_s \eta_r^2 F_r)$$

where s and r indices refer to the sample and reference, respectively, A is the absorbance at λ_{exc}, η is refractive index of the solution, and F is the integrated area of the corrected emission spectrum.[19]

2PA cross-sections (σ) of the samples were obtained using the two-photon excited fluorescence (TPEF) method.[23, 24] by exciting the sample with a Ti:Sapphire femtosecond laser pulse with a repetition rate of 80 MHz and a pulse width of 100 fs in all the laser tuning range from 700 to 1000 nm. The power used to excite the sample is 750 mW with an average power density on the optical elements of 10^{-2} kW cm^{-2} which is low enough to avoid thermooptical distortion of the laser beam.

The samples were dissolved in toluene at a concentration of 1.0×10^{-5} M and the two-photon induced fluorescence intensity was measured at 700-1000 nm by using fluorescein (8.0×10^{-5} M, aqueous NaOH solution, pH 11) as the reference. The 2PA cross-section was calculated by using the following equation:

$$\sigma = \sigma_r \frac{F_S \Phi_r c_r \eta_r}{F_r \Phi_S c_S \eta_S}$$

where s and r indices refer to the sample and reference, σ is the 2PA cross-section value, c is the concentration of the solution, η is the refractive index of the solution, F is the TPEF integral intensities of the solution emitted at the exciting wavelength, and Φ is the fluorescence quantum yield. The σ_r value of reference was taken from the literature.[25]

Incubation and staining of living cells

Cancer cell lines (breast cancer cells, MCF7 and hepatcarcinoma carncer cells, HLF) were maintained in Dulbecco's modified Eagle's medium (DMEM) supplemented with fetal bovine serum (FBS) (10%) penicillin (100 U/mL culture medium), streptomycin (100 μg/mL culture medium), glutamine (5%). Cells were grown in a humidified incubator at 37°C, 5% CO_2, and 95% relative humidity. Cell lines were serum-starved for 24 h before any test.

For staining experiments MCF-7 (5×10^4) was seeded onto 35 mm glass bottom petri dish and incubated in complete media for 24 h. Then, the cells were incubated with the **TK** fluorescent probes at a concentration of 2.0 μM for 60 min in the dark in a humidified incubator at 37°C, 5% CO_2, and 95% relative humidity. After rinsing with phosphate buffered saline (PBS) twice, cells were imaged under confocal microscopy immediately adding complete media without red phenol.

Co-localization in living cells

For the co-localization experiments, living cells were first incubated with dyes for 60 min, then stained with 0.1 μM **MTR** for 30 min or 0.075 μM **LTR** for 60 min. All samples were also stained with Hoechst 33342 (0,2 μM) for 5 min to check the nuclei morphology. The concentration and labeling conditions of each tracker was suggested by manufacturer. For each experiment, the cells were washed every times to remove the unbound probe before staining with another probe. Also for colocalization study after rinsing with PBS twice, cells were imaged under confocal microscopy immediately adding complete media without red phenol.

One-photon/two-photon fluorescence imaging in cells

Biological imaging tests were carried out with a Zeiss LSM700 confocal microscope equipped with an Axio Observer Z1 (Zeiss), inverted microscope using an objective 100X, with 1.46 numerical aperture oil immersion lens for imaging. Laser beams with 405 nm, 488 nm and 542 nm excitation wavelengths were used for Hoechst, TK dyes and commercial trackers imaging, respectively. The fluorescence of dyes was collected through the FITC filter (excitation: 488 nm); the fluorescence of MitoTracker Red- and LysoTracker Red was collected through the TRITC filter (excitation: 550 nm). Images of living cells were also acquired using a Leica Multi Photon confocal scanning system mounted on the Leica TCS SP5 (Leica Microsystem GmbH) and equipped with a 40X oil immersion objective. Cancer cell lines (5×10^4) were seeded onto 35 mm glass bottom Petri Dish and incubated over night. The cells were incubated with the fluorescent dye at a concentration of 1 μg/ml for 1 hours in the dark in a humidified incubator at 37°C, 5% CO2, and 95% relative humidity. An excitation wavelength of 800 nm was used.

For both fluorescence imaging the cells were then rinsed with complete media without red phenol and the images were examined under one or two photon confocal microscope.

Effects of FCCP on uptake of dyes

MCF-7 cells were treated with 10 μM DMSO or 10 μM carbonyl cyanide 4-(trifluoromethoxy)phenylhydrazone (FCCP). Thirty minutes after the treatment the cells were stained with 0.1 μM MitoTracker Red CXMRos or 2.0 μM **TK-Mito1** or **TK-Mito2**. After washing with PBS cells were imaged under confocal microscopy.

Cytotoxicity determination by the MTT method

MCF-7 and HLF cancer cell lines were used in the general cytotoxicity test. The MTT method was used to measure the activity of living cells via mitochondrial dehydrogenase activity. The key component is 3-[4,5-dimethylthiazol-2-yl]-2,5-diphenyltetrazolium bromide or MTT. Mitochondrial dehydrogenases of viable cells cleave the tetrazolium ring, yielding purple MTT formazan crystals, which are insoluble in aqueous solutions. 20 μl of dyes were diluted with complete culture medium. The MTT method is most effective when cultures are prepared in multiwell plates. Cells (10^4 cells/mL) were added to 12-well culture plates at 1000 μL/well, serum-

starved for 24h, and incubated at 37°C in 5% CO2, 95% relative humidity for 24 up to 120 hours, with the **TK** dyes suspension. The control was a complete culture medium. After an appropriate incubation period, cultures were removed from incubator and a MTT solution (10% of the culture volume) was aseptically added. Cultures were returned to incubator and incubated for 3 hours. After the incubation period, cultures were removed from incubator and the resulting MTT formazan crystals were dissolved in DMSO (using the same volume of the culture). The plates were ready within 15 minutes after adding DMSO. After the incubation time, pipetting up and down was required to completely dissolve the MTT formazan crystals. Absorbance at wavelength of 570 nm was measured using the ELISA plate reader. Results were expressed as mean ± S.D. of three separate trials.

Computational details

All calculations have been carried out with the TURBOMOLE[26] program package. Ground state calculations and geometry optimizations were performed using the BLOC functional.[27][28]. Time-dependent calculations were carried out with the BHLYP functional.[29] In all calculations a def2-TZVP basis set[30] was employed.

Synthesis

3,6-dibromo-9H-fluoren-9-one (1) was synthesized following the literature procedure.[31]

3,6-bis(diphenylamino)-9H-fluoren-9-one (TK-Lyso) was synthesized following the literature procedure.[32]

A mixture of 3,6-dibromo-9-fluorenone (0.400 g, 1.18 mmol), diphenylamine (0.440 g, 2.6 mmol) and sodium tert-buthoxide (0.288 g, 3 mmol) was added to suspension of Pd(dba)2 (0.068 g, 0.120 mmol) and PtBu3 (0.180 mL, 0.18 mmol, 1M in toluene) in anhydrous and deoxygenated toluene (5 mL), previous stirred under argon for 10 min. The resulting solution was heated under microwave irradiation at a constant temperature of 110°C for 50 min. The solvent was removed, and the residue was dissolved in dichloromethane and filtered off on short celite column. The solvent was removed by rotary evaporation, and the residue was purified by column chromatography (silica gel, 50:50 hexane, CH2Cl2) to give the product as an orange solid (0.424 g, 70%). ^{1}H-NMR (400 MHz, CDCl3) δ 7.481 (d, J = 8.18 Hz, 2H) 7.29 (m, 8H) 7.11 (m, 12H) 7.02 (d, J = 2 Hz, 2H) 6.78 (dd, J = 2, 8.18 Hz, 2H); ^{13}C-NMR (100 MHz, CDCl3) δ 190.7, 153.2, 146.5, 145, 129.4, 128.3, 125.4, 124.95, 124.2, 121.1, 113.1. MS (APCI) : calcd. for $C_{37}H_{26}N_2O$ 514.02; found: m/z = 515,1 [M+H]$^+$.

N,N-diphenyl-4-(tributylstannyl)aniline (2) was synthesized following the literature procedure.[33]

4-ethynyl-N,N-diphenylaniline (3). Synthetic procedure and characterization has been previously reported.[34]

3,6-bis(4-(diphenylamino)phenyl)-9H-fluoren-9-one (TK-Mito1).

A solution of N,N-diphenyl-4-(tributylstannyl)aniline (**2**) (1.45 g, 2.71 mmol) and 3,6-dibromofluorenone 1 (0.363 g, 1.13 mmol) in 50 mL of DMF and Toluene (1:1) was degassed

under argon for 30 minutes, then Pd(PPh₃)₄ (66 mg, 0.056 mmol) was added. The resulting solution was stirred for 24 h at 85 °C. The mixture was cooled to room temperature then poured into a large amount of water and extracted with methylene chloride. The organic layer was washed with brine and dried over anhydrous Na_2SO_4. The solvent was evaporated under reduced pressure and the resulting residue was purified with column chromatography on silica gel with petroleum ether:ethyl acetate (7:3) as the eluent, to afford the dye TK-Mito1 as an orange solid (70%). ^{1}H NMR (400 MHz, CDCl₃) δ (ppm): 7.77 (s, 1H), 7.76 (d, 1H, J = 1.1 Hz, 1H), 7.73 (s, 1H), 7.71 (d, J = 7.7 Hz, 1H), 7.66-7.60 (m, 4H), 7.55 (d, J = 8.7 Hz, 3H), 7.49 (dd, J_1 = 7.7, J_2 = 1.4 Hz, 1H), 7.45-7.39 (m, 6H), 7.33-7.26 (m, 5H), 7.20 – 7.13 (m, 7H), 7.12 (s, 1H), 7.11-7.05 (m, 2H), 7.07 (s, 1H). 13C NMR (100 Hz, CDCl₃) δ (ppm): 188.6, 148.2, 147.2, 146.9, 144.7, 143.1, 134.6, 133.7, 132.9, 130.3, 129.2, 128.8, 128.2, 127.7, 127.0, 125.3, 124.6, 124.5, 123.2, 122.9, 118.2. MS (APCI) : calcd. for $C_{49}H_{34}N_2O$ 666.81; found: m/z = 667.27 $[M+H]^+$.

3,6-bis[(4-(diphenylamino)phenyl)ethynyl]-9H-fluoren-9-one (TK-Mito2). 3,6-dibromofluorenone **1** (170 mg, 0.50 mmol) and 4-ethynyl-N,N-diphenylaniline (**3**) (269 mg, 1.00 mmol) were dissolved in 5 mL of a mixture of TEA/DMF (1:5). The resulting solution was degassed under argon for 30 min, then Pd(PPh₃)₄ (30 mg, 0.025 mmol) and CuI (10 mg, 0.025 mmol) were added. The resulting mixture was heated under microwave irradiation at a constant temperature of 110°C for 50 min. The solvent was removed, the residue was dissolved in dichloromethane and filtered off on a short celite column. The solvent was removed by rotary evaporation and the residue was purified by column chromatography (silica gel, 50:50 hexane:CH₂Cl₂) to give the dye **TK-Mito2** as an orange solid, 94%. ^{1}H-NMR (400 MHz, CDCl₃) δ 7.66 (s, 2H), 7.64 (dd, J_1 = 7.7, J_2 = 0.5 Hz, 2H), 7.44 (dd, J_1 = 7.6, J_2 = 1.3 Hz, 2H), 7.40 (d, J = 8.8 Hz, 4H), 7.34-7.27 (m, 8H), 7.16-7.11 (m, 8H), 7.12-7.06 (m, 4H), 7.02 (d, J = 8.8 Hz, 4H). ^{13}C-NMR (100 MHz, CDCl₃) δ 192, 148.4, 146.6, 143.6, 133.5, 132.6, 132.1, 130.0, 129.3, 125.1, 124.1, 123.7, 122.9, 121.63, 114.7, 93.7, 88.3. MS (APCI): calcd. for $C_{53}H_{34}N_2O$ 714,27; found: m/z = 715.4 $[M+H]^+$.

Results and discussion

Synthesis

The new fluorenone-based fluorescent probes **TK** were prepared following the synthetic route reported in Scheme 1. Compound **1** was synthesized following the literature procedure.[31] **TK-Lyso** was prepared by a C-N cross-coupling reaction between compound 1 and diphenylamine, in the presence of Pd(dba)₂ (dba = dibenzylideneacetone) and P(tBu)₃ as the catalytic system, for 60 minutes in a microwave reactor.[32] **TK-Mito1** was prepared via the Stille reaction between reagents **1** and **2**, in the presence of Pd(Ph₃)₄ in toluene, while **TK-Mito2** was synthesized by the Sonogashira reaction of **1**

with **3**, in the presence of Pd(PPh₃)₄ and CuI as the catalytic system, for 60 minutes in a microwave reactor.

Photophysical properties of TK

The optical properties of **TK-Lyso**, **TK-Mito1** and **TK-Mito2** were studied in five solvents with different polarities as shown in Table S5. The absorption and emission spectra of **TK** dyes in toluene are reported in Fig. 1, while those recorded in others solvents are reported in the supporting data (Table S5). Two major absorption bands can be observed, the first at about 305 nm, attributed to π-π* transition of diphenylamine and triphenylamine units, the second at about 400-460 nm, assigned as the intramolecular charge transfer (ICT) absorption band. This band shows a regular red shift in all tested solvents. As shown in Table S1, the fluorescence quantum yields of the three probes in water ($\Phi_{TK-Lyso}$ = 0.07, $\Phi_{TK-Mito1}$ = 0.043 and $\Phi_{TK-Mito2}$ = 0.018) were much lower than those in hydrophobic toluene. These results indicated that the strong fluorescence of **TK** dyes could be observed in hydrophobic enviroments, for example, $\Phi_{TK-Lyso}$ = 0,49, $\Phi_{TK-Mito1}$ = 0,54 and $\Phi_{TK-Mito2}$ = 0,59 in toluene.

By comparing the absorption and emission spectra, large Stokes shifts of 73, 93 and 113 nm were observed for three dyes, **TK-Lyso**, **TK-Mito1** and **TK-Mito2**, respectively. Thus **TK** fluorophores with low background signals seem suitable for staining of hydrophobic biomembrane, such as those **Mito** and **Lyso** organelles.[35] The fluorescence and absorption intensities of **TK** dyes remained stable at pH 2.0-9.0, suggesting that all the probes were pH independent (Fig. S6).
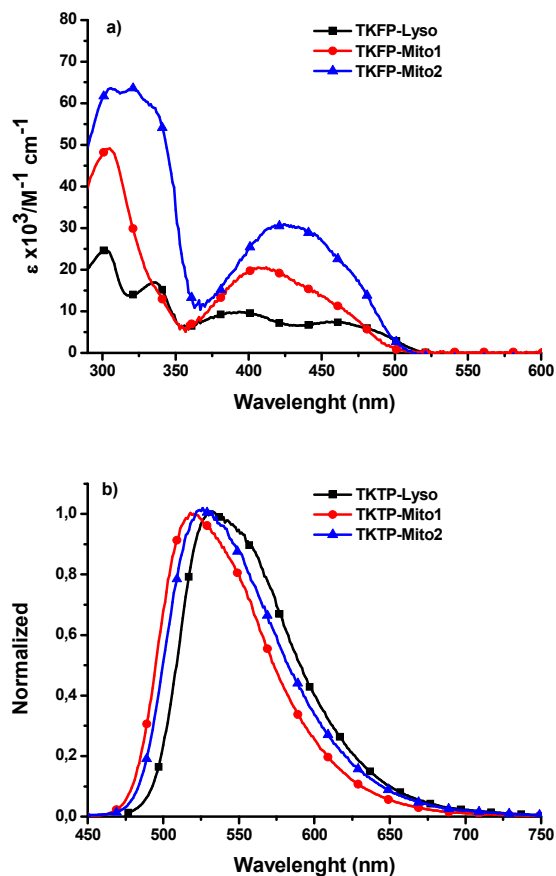
Fig. 1 The optical properties of **TKTP-Lyso**, **TKTP-Mito1** and **TKTP-Mito2**. (a) Absorption of dyes in toluene. (b) Normalized fluorescence od dyes in toluene.

Upon two-photon excitation at 800 nm by the femtosecond laser pulse in toluene, a fluorescence at round 540-590 nm is observed, (Fig. S3). The log-log plots of the fluorescence intensity versus pumped power (Fig. 2) show linear behaviours with slope of 1.82, 1.84 and 1.80, respectively for **TK-Lyso**, **TK-Mito1** and **TK-Mito2**, demostrating that in these fluorenone-derivatives two-photon excitation processes are activated.

The two-photon cross section (σ) was determined by the two-photon-induced fluorescence measurement technique as described previously.[36] The two-photon cross section (σ) of chromophores **TK** were measured in the wide wavelength range from 700-1000 nm. Furthermore, two-photon action cross-section ($\sigma\Phi$) are shown in Fig. 3, showing a maximum value of $\approx$ 520 GM **TK-Mito2**, $\approx$ 300 GM for **TKMito1** and $\approx$ 150 GM for **TK-Lyso**.
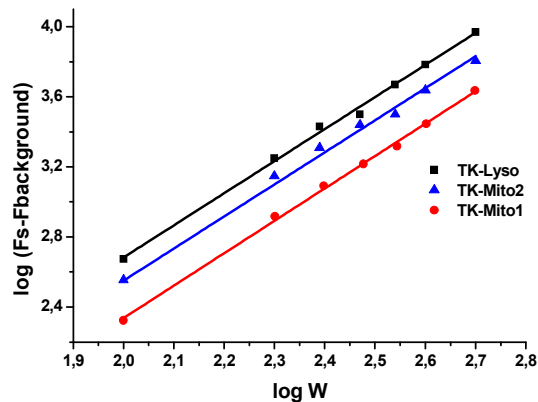

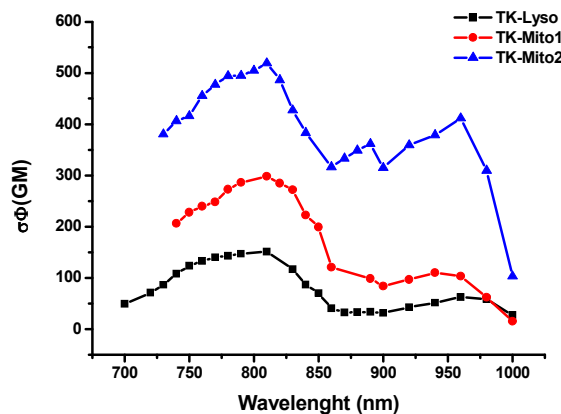**Fig. 2** The log-log plot of the emission intensity versus incident power of TK-Lyso, TK-Mito1 and TK-Mito2

Fig. 3 Two-photon action absorption cross-section (σ, 1 GM = 10^{-50} cm^4 s per photon per molecule) of **TK-Lyso**, **TK-Mito1** and **TK-Mito2** in toluene versus excitation wavelengths of an identical power of 0.75 W

To aid the assignment of transitions in the absorption spectrum TD-DFT calculations have been performed on the dyes. The results are reported in Table 1.

The computed energies are in reasonable agreement with the experimental results, showing that all dyes display absorption around 400-500 nm as well as at about 350 nm.

Nevertheless, despite all excitations are, in general, of π-π^* character, they show non-negligible differences concerning their localization. Inspection of Table 1 shows in fact that the absorption peak at 400-500 nm is originated, in all dyes, by two excited states characterized by the HOMO->LUMO and HOMO-1->LUMO single-particle transitions, respectively. These excitations display intramolecular charge-transfer (ICT) (see Fig.4 for a plot of the relevant molecular orbitals), where the charge is moved towards the central backbone of the molecule upon photon absorption. On the other hand, the excitations with energies around 340-360 nm have different features. In **TK-Lyso** this is characterized by a HOMO-2 ->

LUMO single-particle transition which is mainly localized on the central backbone of the molecule with no appreciable ICT.

In **TK-Mito1** and **TK-Mito2** the excitations at about 350-360 nm have an ICT signature, involving mainly a HOMO -> LUMO+1 transition, so that a photoinduced ICT to the central backbone of the molecule can be observed. In **TK-Mito2** this behavior is even reinforced by the presence of a second excited state, characterized by a HOMO-1 -> LUMO single-particle transition, with high oscillator strength and very close in energy to the previous one.

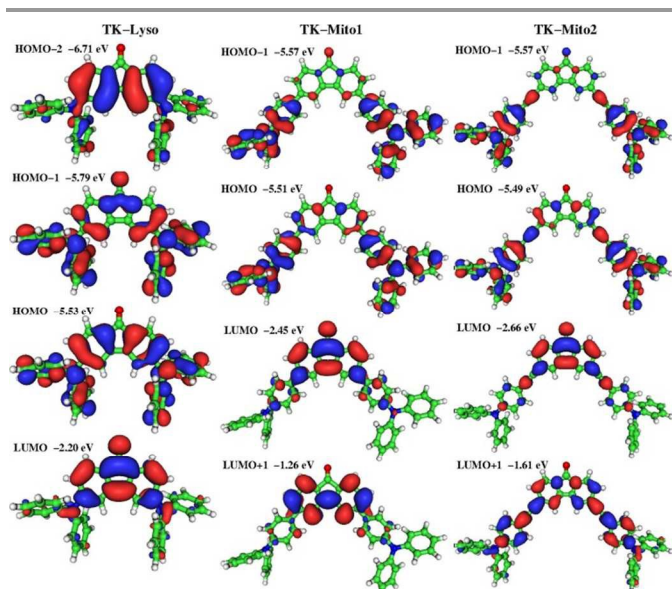**Fig. 4** Molecular orbital energy of **TK** dyes.

Table 1. Lowest singlet excitation energies, oscillator strengths (o.s.) and single particle transitions for the different dyes.

Dye	Energy (nm)	o.s.	transition
TK-Lyso	477	0.204	H-> L (97%)
	398	0.183	H-1 -> L (97%)
	389	0.002	H-3 -> L (95%)
	368	0.023	H-> L+1 (70%)
	340	0.354	H-2 -> L (68%)
TK-Mito1	488	0.371	H-> L (95%)
	452	0.222	H-1 -> L (99%)
	399	0.001	H-5 -> L (88%)
	389	0.031	H-2 -> L (87%)
	343	0.213	H -> L+1 (70%)
TK-Mito2	527	0.759	H-> L (95%)
	477	0.373	H-1 -> L (99%)
	408	0.000	H-5 -> L (94%)
	403	0.016	H-2 -> L (81%)
	362	0.908	H-1 -> L (75%)
	361	0.628	H-> L+1 (90%)

Imaging in living cells

In order to assess the staining ability of **TK** dyes in living cells, MCF-7 were incubated in complete culture medium and the uptake was studied by confocal microscopy at different time point from 1 hour up to 4 days. Upon one-photon excitation, the fluorescence of the dyes clearly confirmed that our molecules efficiently stain the cells, penetrating the cell membrane reaching the cytoplasm within 60 min. (Fig. 5).

Thanks to excellent light fastness and low toxicity, **TK** dyes are also well suitable for long-term fluorescence imaging experiments. Furthermore, intracellular long time retention is another important feature for probe, especially for tracers. Consistent with the results shown in Fig 6, no background fluorescence was observed, which again confirmed the ability of **TK** dyes to penetrate membranes and easily enter cells. Confocal microscopy results for living MCF-7 cells showed that the staining pattern remained the same with a strong fluorescence in the cytoplasm and the a total fluorescence intensity in cells almost unchanged for at least five days after removing the dyes from culture media. In particular, no fluorescence was observed in extracellular regions, indicating that dyes loaded within living cells did not leaked.
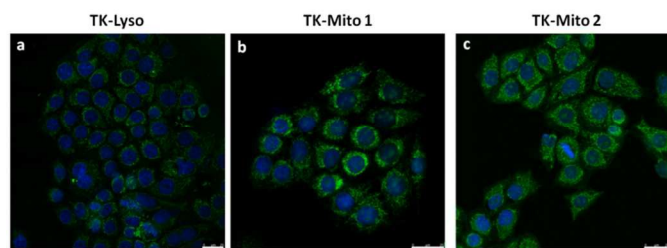
Fig. 5 Staining green pattern of **TK-Lyso** 2.0 µM (a), **TK-Mito1** 2.0 µM (b) and **TK-Mito2** 2.0 µM (c) in MCF7 cells measured by confocal microscopy after 1 hour of incubation. Nuclei were stained with Hoechst 33342 (0,2 µM). Scale bar, 25 µm.
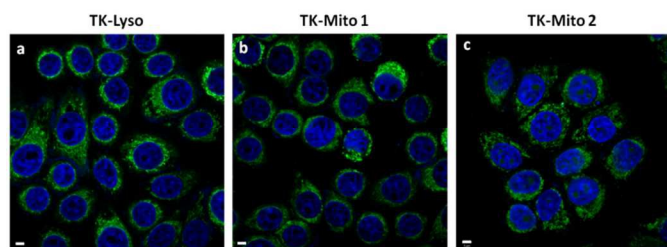

Fig. 6 Permanent green staining of of **TK-Lyso** 2.0 µM (a), **TK-Mito1** 2.0 µM (b) and **TK-Mito2** 2.0 µM (c) in MCF7 cells measured by confocal microscopy after five days. Nuclei were stained with Hoechst 33342 (0,2 µM). Scale bar, 5 µm.

Co-localization in living cells

Studying confocal micrographs we observed that our probes stained some organelles in the cytoplasm. Take in account the different chemical structure and different polarity, we expected a different subcellular localization of **TK** dyes.

As it is well-known, the co-staining experiments with a commercial probe are a common method to detect the selectivity of a new probe, while the prerequisite of co-localization experiments is that no optical and chemical interferences exists between the two dyes. Only live cell imaging gives an accurate picture of the intracellular location of probes. The commercially available mitochondria-specific staining probe, MitoTracker Red (**MTR**) and lysosomes-specific staining probe, LysoTracker Red (**LTR**), were co-incubated with dyes. This was accomplished by first incubating cells with **TK** dyes, as described above, and then with **LTR** or **MTR**, in order to label lysosomes or mitochondria, respectively.

TK dyes were excited at 488 nm, while **MTR** or **LTR** were excited at 555 nm. By exciting at 488 nm the fluorescence of **MTR** or **LTR** doesn't interfere with the fluorescence of **TK** dyes. Thus, **MTR** will be utilized in further experimental investigation in the staining of mitochondria with **TK-Mito1** and **TK-Mito2**, while **LTR** will be utilized in the staining of lysosomes with **TK-Lyso**. Moreover, to prevent any problem concern with the overlapping of spectra we perform confocal imaging experiments exciting first the commercial dye and then our probes.
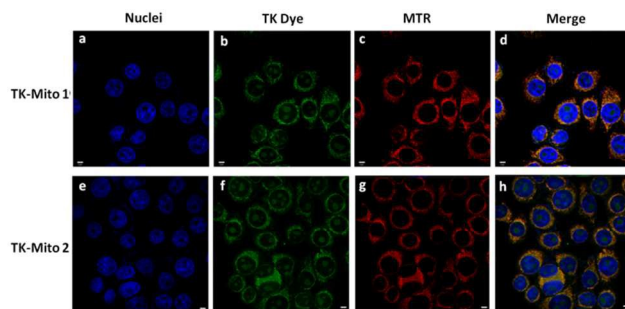

Fig. 7 TK Mito1 (a-d) and **TK-Mito2** (e-h) colocalization study: (a, e) nuclei stained with Hoechst 33342 (0,2 µM), λex 405 nm and light collection range 420-1000 nm; (b, f) TK dyes 2.0 µM, λex 488 nm and light collection range 493-1000 nm; (c, g) commercial Mitotracker-red 0.1 µM, λex 555 nm and light collection range 560-1000 nm ; (d, h) merge of three previous images. Scale bar, 5 µm.
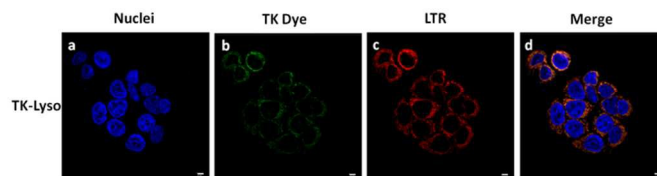

Fig. 8 TK-Lyso colocalization study: (a) nuclei stained with Hoechst 33342 (0,2 µM),), λex 405 nm; (b) TK dye 2.0 µM, λex 488 nm and light collection range 493-1000 nm; (c) commercial Lysotracker-red 0.1 µM, λex 555 nm and light collection range 560-1000 nm; (d) merge of three previous images. Scale bar, 5 µm.

The merge of the two images was made after acquisition by software, allowing also the study of the overlapping coefficient of two fluorescent channels.

The study of the subcellular distribution of **TK** dyes through commercial markers, confirmed that two of them, **TK-Mito1** and **TK-Mito2,** co-localize with mitochondria and only one, **TK-Lyso,** co-localize with lysosomes. In particular, as shown in confocal pictures, clearly the dyes are able to enter inside cells with no apparent surface binding on the cellular membrane. Fig. 7 displays co-localization of **TK-Mito1** and **TK-Mito2** with MitoTracker Red, in the merge image the yellow areas indicate the overlap regions. It is encouraging to see that most of the green converge to yellow, indicating that the majority of **TK-Mito1** and **TK-Mito2** is in the same location of the cell as the **MTR**.

On the contrary Fig. 8 displays co-localization of **TK-Lyso** with LysoTracker Red. The merge (fig.6d) shows that the co-localization, so the overlap of green fluorescence and red one, of our dye with lysosomes is very relevant. Moreover, the **TK** dyes are co-localized and they not label other parts of the cell, such as the nucleus. Furthermore, to quantify the amount of co-localization of dyes was used the Pearson's sample correlation factors (R_r). Results evidenced that for **TK-Mito1** and **TK-Mito2** with **MTR** co-localizing pixels are 85% and 94% of the total, respectively; while the co-localizing pixels of **TK-Lyso** with LTR are equal to 89%.

Effects of FCCP on uptake of dyes

The staining of **TK** dyes in MCF-7 cells treated with a membrane-potential uncoupler was examined. The uncoupler, carbonyl cyanide 4-(trifluoromethoxy) phenylhydrazone (FCCP), can disrupt mitochondrial membrane potential (Fig. 9). Staining with MitoTracker Red CXMRos, whose mitochondrial uptake is dependent on mitochondrial membrane potential, was decreased in the presence of FCCP,[37, 38] to a level lower than that in the DMSO control.
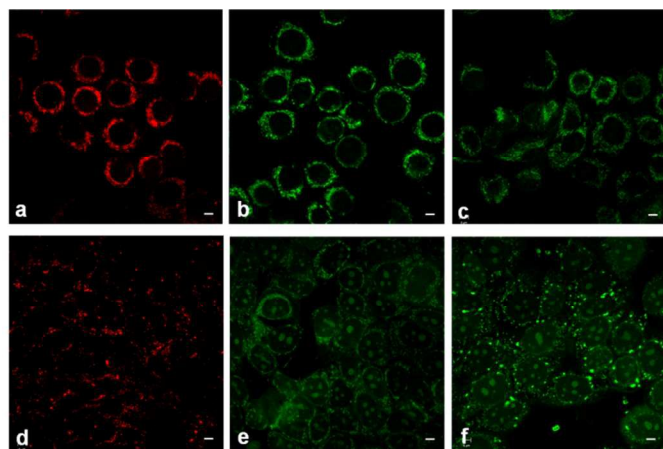

Fig. 9 Staining patterns of **TK-Mito1**, **TK-Mito2** and MitoTracker Red in MCF-7 cells. The cells were incubated in the absence (a-c) or presence of 10 μM FCCP for 30 min, (d-f) then stained with 0.2 μM MitoTracker Red CXMRos for 30 min, or 15 min, and 2.0 μM **TK** dyes for 1 h. Scale bar,2 5 μm.

The staining pattern of **TK-Mito1** and **TK-Mito 2** with or without FCCP evidences dependence on the membrane potential.

Two-Photon Fluorescence Imaging in Cells

In the next step, to further demonstrate the potential application of **TK** dyes in living cells we perform two-photon fluorescence microscopy imaging. We carried out spectroscopic studies of MCF-7 living cells stained with **TK-Mito1** and **TK-Mito2** dyes to image intracellular mitochondria, and **TK-Lyso** to image intracellular lysosomes.

Two-photon fluorescence microscopy provides key advantages over one-photon fluorescence imaging, such as, increased penetration depth, lower tissue autofluorescence and self-absorption, reduced photodamage and photobleaching. In two-photon microscopy imaging, the optimal excitation wavelength of each compound was used. Living MCF-7 cells were imaged a 6 mW (this power is safe for living specimens) beam at 800 nm. As shown in Fig. 10 all of the probes in living cells provided enough fluorescence intensity and image resolution. MCF-7 cells showed bright green fluorescence upon excitation. These results highlight the potential of **TK** dyes for both one- and two-photon fluorescence microscopy imaging applications.
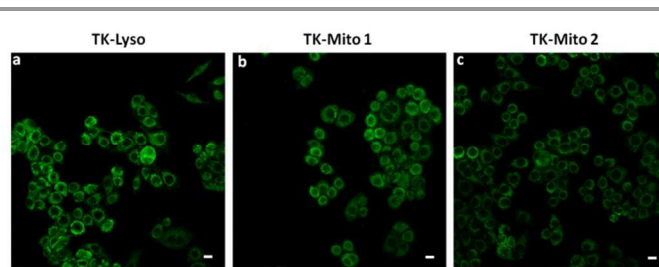

Fig 10 Staining patterns of **TK** dyes 2.0 μM in MCF7 cells obtained with the two-photon fluorescence microscopy. Scale bar, 10 μm

Cytotoxicity

The confocal microscopy showed the absence of mitochondrial membrane damage and cell morphology retention also after some days of culture after dyes treatment. This suggests an almost low toxicity of **TK** dyes. To confirm the observations, the cytotoxicity test was performed using the MTT method. MCF-7 and HLF cells were incubated with **TK** dyes at a concentration 10 times higher than that used in staining experiments. Cell viability was studied in a time-course experiment (Fig. 12) from 24h up to 72h.

In Fig. 13 are reported the all data obtained at different time point for two cell lines. The results clearly indicate that MCF-7 and HLF cells incubated with our dyes remained 99% viable after 72 h of feeding time, demonstrating high biocompatibility of dyes. Within experimental errors, no detectable difference could be discerned between **TK** dyes.
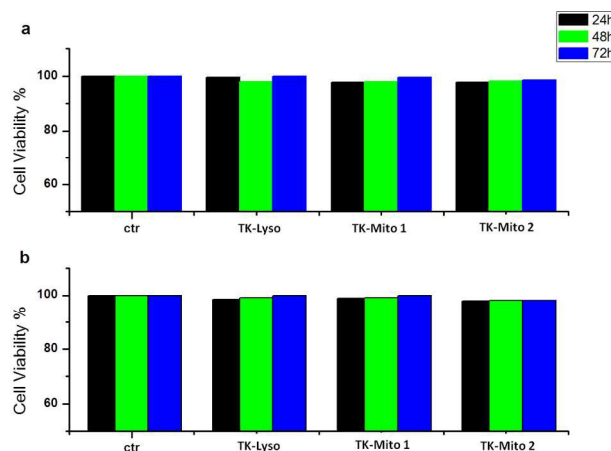

Fig. 11 MTT cytotoxicity tests for MCF-7 (a), HLF (b) cells treated with **TK** dyes compared to untreated cells (Ctr)

Photostability in MCF-7 cell

Under the high-intensity illumination conditions used for fluorescence microscopy, the irreversible destruction of the excited fluorophore (photobleaching) often becomes the factor limiting fluorescence detectability. In order to quantitatively investigate the photostability of **TK** dyes, MCF-7 cells stained with them, **MTR** or **LTR** were exposed to constant laser beam. The fluorescence intensity of intracellular **TK** dyes was normalized and plotted as a function of time. In Fig 10 the dyes

exhibit a slow decrease of fluorescence emission during 10 scans with a total irradiation time of about 30 min. In contrast, the signal intensity of **LTR** and **MTR** quickly decrease. The slight fluctuation of the signal intensity may be due to the metabolic activity of the living cells. These results suggest a superior photostability of **TK** dyes, with respect to the commercial trackers **LTR** and **MTR**.
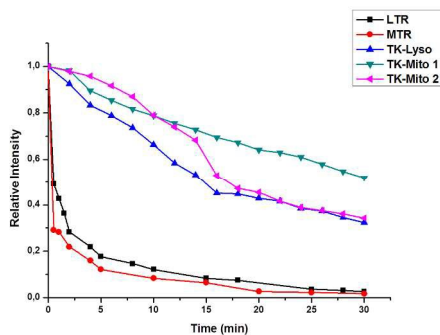

Fig. 12 The fluorescence intensity in MCF-7 cells was determined staining with **TK-Lyso** (2.0 μM), **TK-Mito1** (2.0 μM) and **TK-Mito2** for 60 min, **MTR** (0.1 μM) and **LTR** (0.075 μM for 60 min) by confocal microscopy. The changes of fluorescence intensity in the consecutive t-scan mode were determined for 30 min (time interval of data determination = 2 min). Excitation wavelength for our probes was 488 nm, instead for commercial trackers was 514 nm. Data were obtained from replicate experiments (n = 5).

The fluorescence intensity of intracellular **TK** dyes was normalized and plotted as a function of time. In Fig 10 the dyes exhibited a slow decrease of fluorescence emission during 10 scans with a total irradiation time of about 30 min. In contrast, the signal intensity of LTR and MTR quickly decreased. The slight fluctuation of the signal intensity may be due to the metabolic activity of the living cells. These results suggested a superior photostability of **TK** dyes.

Conclusion

In summary, we synthesized and characterized three fluorenone-derived two-photon fluorescent probes specifically targeting lysosomes (**TK-Lyso**) and mitochondria (**TK-Mito1** and **TK-Mito2**) in cancer cell. These probes showed excellent and superior photostability compared with commercial **LTR** and **MTR** trackers, long-term retention inside the cells, high biocompatibility and low cytotoxicity. **TK** dyes, also showed insensitivity to the pH in the range 4-10, maintaining intact their fluorescence capability. In addition, **TK-Mito1** and **TK-Mito2** revealed independence and dependence of mitochondrial membrane potential, respectively. The results of the present work disclose a new class of organic dyes with potential broad applications as specific and efficient **Lyso** and **Mito** trackers in the studies of various biological processes.

Acknowledgements

Notes and references

a Istituto Nanoscienze – CNR, National Nanotechnology Laboratory (NNL), Via Arnesano, 73100 Lecce, Italy.

b Center for Biomolecular Nanotechnologies (CBN) Fondazione Istituto Italiano di Tecnologia (IIT), Via Barsanti 1, Arnesano, 73010, Italy

c Dipartimento di beni culturali, Università del Salento, Via Monteroni, 73100, Lecce, Italy.

d Istituto di Chimica dei Composti OrganoMetallici (ICCOM) – Consiglio Nazionale delle Ricerche CNR, Via Orabona, 4 – 70125 Bari, Italy.

e Dipartimento di Matematica e Fisica "Ennio De Giorgi", Università del Salento, Via Monteroni, 73100, Lecce, Italy.

f Dipartimento di Ingegneria dell'Innovazione, Università del Salento, Via Monteroni, 73100, Lecce, Italy.

1. B. A. D. Neto, P. H. P. R. Carvalho, D. C. B. D. Santos, C. C. Gatto, L. M. Ramos, N. M. d. Vasconcelos, J. R. Correa, M. B. Costa, H. C. B. de Oliveira and R. G. Silva, *RSC Advances*, 2012, **2**, 1524-1532.

2. B. A. D. Neto, J. R. Correa and R. G. Silva, *RSC Advances*, 2013, **3**, 5291-5301.

3. S. R. Adams, A. T. Harootunian, Y. J. Buechler, S. S. Taylor and R. Y. Tsien, *Nature*, 1991, **349**, 694-697.

4. W. Yin, H. Zhu and R. Wang, *Dyes and Pigments*, 2014, **107**, 127-132.

5. A. Gomes, E. Fernandes and J. L. F. C. Lima, *Journal of Biochemical and Biophysical Methods*, 2005, **65**, 45-80.

6. K. P. Carter, A. M. Young and A. E. Palmer, *Chemical Reviews*, 2014, **114**, 4564-4601.

7. Y. Gabe, Y. Urano, K. Kikuchi, H. Kojima and T. Nagano, *Journal of the American Chemical Society*, 2004, **126**, 3357-3367.

8. P. J. Hrdlicka, B. R. Babu, M. D. Sørensen, N. Harrit and J. Wengel, *Journal of the American Chemical Society*, 2005, **127**, 13293-13299.

9. C.-N. Im, N.-Y. Kang, H.-H. Ha, X. Bi, J. J. Lee, S.-J. Park, S. Y. Lee, M. Vendrell, Y. K. Kim, J.-S. Lee, J. Li, Y.-H. Ahn, B. Feng, H.-H. Ng, S.-W. Yun and Y.-T. Chang, *Angewandte Chemie*, 2010, **122**, 7659-7662.

10. M. Vendrell, J.-S. Lee and Y.-T. Chang, *Current Opinion in Chemical Biology*, 2010, **14**, 383-389.

11. P. B. Gahan, *Cell Biochemistry and Function*, 2005, **23**, 222-222.

12. A. T. Hoye, J. E. Davoren, P. Wipf, M. P. Fink and V. E. Kagan, *Accounts of Chemical Research*, 2008, **41**, 87-97.

13. L. F. Yousif, K. M. Stewart and S. O. Kelley, *ChemBioChem*, 2009, **10**, 1939-1950.

14. J. Nunnari and A. Suomalainen, *Cell*, 2012, **148**, 1145-1159.

15. J. Bereiter-Hahn, M. Vöth, S. Mai and M. Jendrach, *Biotechnology Journal*, 2008, **3**, 765-780.

16. W. Denk, J. Strickler and W. Webb, *Science*, 1990, **248**, 73-76.

17. W. Kaiser and C. G. B. Garrett *Phys. Rev. Lett.*,1961, **7**, 229–231 .

18. H. C. Gerritsen and C. J. De Grauw, *Microscopy Research and Technique*, 1999, **47**, 206-209.

19. W. Yang, P. S. Chan, M. S. Chan, K. F. Li, P. K. Lo, N. K. Mak, K. W. Cheah and M. S. Wong, *Chemical Communications*, 2013, **49**, 3428-3430.

20. H. Zhang, J. Fan, H. Dong, S. Zhang, W. Xu, J. Wang, P. Gao and X. Peng, *Journal of Materials Chemistry B*, 2013, **1**, 5450-5455.

21. X. Wang, D. M. Nguyen, C. O. Yanez, L. Rodriguez, H.-Y. Ahn, M. V. Bondar and K. D. Belfield, *Journal of the American Chemical Society*, 2010, **132**, 12237-12239.

22. F. Miao, W. Zhang, Y. Sun, R. Zhang, Y. Liu, F. Guo, G. Song, M. Tian and X. Yu, *Biosensors and Bioelectronics*, 2014, **55**, 423-429.

23. G. A. Crosby and J. N. Demas, *The Journal of Physical Chemistry*, 1971, **75**, 991-1024.

24. S. K. Lee, W. J. Yang, J. J. Choi, C. H. Kim, S.-J. Jeon and B. R. Cho, *Organic Letters*, 2004, **7**, 323-326.

25. C. Xu and W. W. Webb, *J. Opt. Soc. Am. B*, 1996, **13**, 481-491.

26. TURBOMOLE V6.4 2012, a development of University of Karlsruhe and Forschungszentrum Karlsruhe GmbH, 1989–2007, TURBOMOLE GmbH, since 2007; available from http://www.turbomole.com.

27. L. A. Constantin, E. Fabiano and F. Della Sala, *Journal of Chemical Theory and Computation*, 2013, **9**, 2256-2263.

28. L. Constantin, E. Fabiano and F. Sala, *Physical Review B*, 2012, **86**, 035130.

29. A. D. Becke, *The Journal of Chemical Physics*, 1993, **98**, 1372-1377.

30. F. Weigend, M. Haser, H. Patzelt and R. Ahlrichs, Chem. Phys. Lett., 1998, 294, 143.

31. B. Kobin, L. Grubert, S. Blumstengel, F. Henneberger and S. Hecht, *Journal of Materials Chemistry*, 2012, **22**, 4383-4390.

32. A. L. Capodilupo, L. De Marco, E. Fabiano, R. Giannuzzi, A. Scrascia, C. Clarlucci, G. A. Corrente, M. P. Cipolla, G. Gigli and G. Ciccarella, *Journal of Materials Chemistry A*, 2014, **2**, 14181-14188.

33. M. Yang, X. Chen, Y. Zou, C. Pan, B. Liu and H. Zhong, *J Mater Sci*, 2013, **48**, 1014-1020.

34. A. Scrascia, M. Pastore, L. Yin, R. Anna Picca, M. Manca, Y.-C. Guo, F. De Angelis, F. Della Sala, R. Cingolani, G. Gigli and G. Ciccarella, *Current Organic Chemistry*, 2011, **15**, 3535-3543.

35. G. Signore, R. Nifosì, L. Albertazzi, B. Storti and R. Bizzarri, *Journal of the American Chemical Society*, 2010, **132**, 1276-1288.

36. M. Rumi, J. E. Ehrlich, A. A. Heikal, J. W. Perry, S. Barlow, Z. Hu, D. McCord-Maughon, T. C. Parker, H. Röckel, S. Thayumanavan, S. R. Marder, D. Beljonne and J.-L. Brédas, *Journal of the American Chemical Society*, 2000, **122**, 9500-9510.

37. Y. Kawazoe, H. Shimogawa, A. Sato and M. Uesugi, *Angewandte Chemie International Edition*, 2011, **50**, 5478-5481.

38. S. Versari, A. M. Villa, A. Villa, S. M. Doglia, G. A. Pagani and S. Bradamante, *BIOMEDO*, 2006, **11**, 034014-034014-034014.

Three fluorenone-based two-photon fluorescent probes for specific targeting of lysosomes and mitochondria in cancer cell.